J. Am. Chem. Soc. **1986**, *108*, 5426–5433

The Ordering of Benzyl Alcohol and Its Influence on Phospholipid Order in Bilayer Membranes

J. M. Pope,[†] D. Dubro,[†] J. W. Doane,*[†,‡] and P. W. Westerman[⊥]

Contribution from the School of Physics, The University of New South Wales, P.O. Box 1, Kensington N.S.W. 2033, Australia, and the Department of Biochemistry and Molecular Pathology, Northeastern Ohio Universities College of Medicine, Rootstown, Ohio 44272.
Received April 15, 1985

Abstract: ^{2}H NMR measurements on several dimyristoylphosphatidylcholine (DMPC)/water/benzyl alcohol (BZA) ternary systems in the L_α phase are reported. The results on selectively deuterated BZA are analyzed on the basis of several possible models for the conformational motion of the benzene ring with respect to the α-hydroxymethyl group. The data are not consistent with a model in which the ring rotates rapidly relative to the hydroxymethyl group about the para axis of the molecule. Results for selectively deuterated DMPC show that at a molar ratio BZA:DMPC of 7:15, BZA has its greatest effect on the orientational ordering of the head group and glycerol moiety in the "backbone" region of the bilayer membranes. This confirms the location of the molecule in the interfacial region of the bilayer. The NMR data are supported by low-angle X-ray diffraction measurements which show significant increases in bilayer area per lipid molecule on incorporation of BZA in the membrane.

It is still unclear how and where anesthetics exert their pharmacological effects on excitable tissues and produce the physiological phenomenon known as anesthesia.[1-7] Anesthesia can be induced by reagents ranging from xenon to steroids, suggesting a molecular mechanism that involves a nonspecific receptor site. The excellent correlation of lipid solubility with anesthetic potency[1] implies an interaction with hydrophobic regions in the membrane and has led to the formulation of various unitary theories of anesthesia. These theories propose that all general anesthetics act by the same mechanism at a common molecular and subcellular site. There have been numerous suggestions as to the precise location of this site within the cell. Although it is widely agreed that the ultimate effects of general anesthetics are on proteins, the following question remains: do anesthetics act directly on proteins or do they act indirectly by first affecting membrane lipids or cellular water?[8,9] Unitary theories based on membrane lipids as the site of anesthetic action have been favored.[1] These may be grouped into three broad categories depending on whether they emphasize membrane expansion or thickening, an anesthetic induced phase transition, or changes in fluidity as triggering the onset of anesthesia.[1-6]

As a first step in critically evaluating lipid-based unitary theories of anesthesia, it is necessary to determine the distribution of anesthetic molecules in lipid bilayers and their effect on bilayer structure. Using calorimetric[10-13] dilatometric,[14] and spin label methods,[15,16] a number of authors have studied the effects of anesthetics on lipid structure by examining how they change the chain-melting temperature T_m of the lipids. Changes in bilayer thickness on incorporation of *n*-alkanes have been investigated by means of membrane capacitance measurements,[17] X-ray,[13,18] and neutron[19] diffraction. However, surprisingly little is known about how anesthetic molecules are oriented by, and interact with, phospholipid bilayers at the molecular level. Novak and Swift[20] have demonstrated an interaction between lipid head groups and anesthetic barbiturates in nonpolar solvents by ^{1}H NMR. Halothane and xenon have been shown by ^{19}F and Xe NMR, respectively, to be in fast exchange between the membrane and aqueous phases in some model and biological membranes, but this is not the case with saturated lecithins, even above their phase transition.[21-23] Kelusky and Smith[24-26] have employed ^{2}H NMR to study the binding of procaine and tetracaine to lipid bilayers formed from egg PC and PE (phosphatidylethanolamine). Here too, the anesthetics are in slow exchange between the bilayer and the aqueous phase. Tetracaine partitions strongly into the lipid while procaine is only weakly bound. Recently the interaction of *n*-octanol and *n*-decanol with model membrane systems has been examined by ^{2}H NMR.[27,28]

The effect of the local anesthetic benzyl alcohol (BZA) on bilayer structure has received more attention.[29-37] Ashcroft et

[†] The University of New South Wales.
[‡] On leave from the Liquid Crystal Institute, Kent State University, Kent, Ohio 44242.
[⊥] Northeastern Ohio Universities College of Medicine.

(1) Janoff, A. S.; Miller, K. W. In *Biological Membranes*; Chapman, D. Ed.; Vol. 4, Academic Press: London, 1982; Vol. 4 pp 417–476.
(2) Franks, N. P.; Lieb, W. R. *Nature (London)* **1982**, *300*, 487–493.
(3) Roth, S. H. *Ann. Rev. Pharmacol. Toxicol.* **1979**, *19*, 159–178.
(4) Kaufman, R. D. *Anaesthesiology* **1977**, *46*, 49–62.
(5) Haydon, D. A.; Henry, B. M.; Levinson, S. R. *Nature (London)* **1977**, *286*, 356–358.
(6) Lee, A. G. *Nature (London)* **1976**, *262*, 545–548.
(7) Seeman, P. *Pharmacol. Rev.* **1972**, *24*, 583–655.
(8) Miller, S. L. *Proc. Natl. Acad. Sci. U.S.A.* **1961**, *47*, 1515–1524.
(9) Pauling, L. *Science* **1961**, *134*, 15–21.
(10) Hill, M. W. *Biochim. Biophys. Acta* **1974**, *356*, 117–124.
(11) Eliasz, A. W.; Chapman, D.; Ewing, D. F. *Biochim. Biophys. Acta* **1976**, *448*, 220–233.
(12) Papahadjopoulos, D.; Jacobson, K.; Poste, G.; Shepherd, G. *Biochim. Biophys. Acta* **1975**, *394*, 504–519.
(13) McIntosh, T. J.; Simon, S. A.; MacDonald, R. C. *Biochim. Biophys. Acta* **1980**, *597*, 445–463.
(14) MacDonald, A. G. *Biochim. Biophys. Acta* **1978**, *507*, 26–37.
(15) Pringle, M. J.; Miller, K. W. *Biochemistry* **1979**, *18*, 3314–3320.
(16) Chaykowski, F. T.; Wan, J. K. S.; Singer, M. A. *Chem. Phys. Lipids* **1979**, *23*, 111–123.
(17) Haydon, D. A.; Hendry, B. M.; Levinson, S. R.; Reguena, J. *Biochim. Biophys. Acta* **1977**, *470*, 17–34.
(18) Lea, E. J. A. *Int. J. Biol. Macromol.* **1979**, *1*, 185–187.
(19) White, S. H.; King, G. I.; Cain, J. E. *Nature (London)* **1981**, *290*, 161–163.
(20) Novak, R. F.; Swift, T. J. *Proc. Natl. Acad. Sci. U.S.A.* **1972**, *69*, 640–642.
(21) Trudell, J. R.; Hubbell, W. L. *Anaesthesiology* **1976**, *44*, 202–205.
(22) Koehler, L. S.; Fossel, E. T.; Koehler, K. A. *Biochemistry* **1977**, *16*, 3700–3707.
(23) Miller, K. W.; Reo, N. V.; Shoot Uiterkamp, A. J. M.; Stengle, D. P.; Stengle, T. R.; Williamson, K. L. *Proc. Natl. Acad. Sci. U.S.A.* **1981**, *78*, 4946–4949.
(24) Kelusky, E. C.; Smith, I. C. P. *Biochemistry* **1983**, *22*, 6011–6017.
(25) Kelusky, E. C.; Smith, I. C. P. *Can. J. Biochem. Cell Biol.* **1984**, *62*, 178–184.
(26) Kelusky, E. C.; Smith, I. C. P. *Mol. Pharmacol.* **1984**, *26*, 314–321.
(27) Thewalt, J. L.; Wassell, S. R.; Garrissen, H.; Cushley, R. J. *Biochim. Biophys. Acta* **1985**, *817*, 355–365.
(28) Pope, J. M.; Walker, L. W.; Dubro, D. *Chem. Phys. Lipids* **1984**, *35*, 259–277.
(29) Ashcroft, R. G.; Coster, H. G. L.; Smith, J. R. *Biochim. Biophys. Acta* **1977**, *469*, 13–22.
(30) Ashcroft, R. G.; Coster, H. G. L.; Smith, J. R. *Nature (London)* **1977**, *269*, 819–820.
(31) Reyes, J.; Latorre, R. *Biophys. J.* **1979**, *28*, 259–280.

0002-7863/86/1508-5426$01.50/0

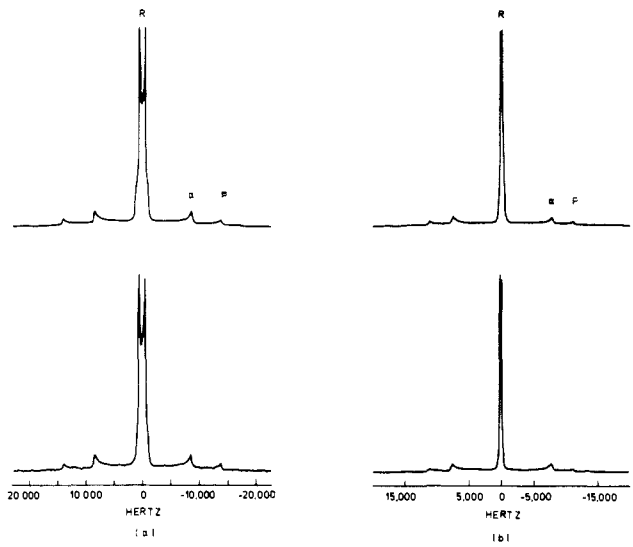

Figure 1. Representative ^2H NMR spectra of BZA(d_7) in lipid bilayer of molar composition DMPC/0.5 BZA/9H_2O for two temperatures in the L_α phase: (a) 21 °C, (b) 42 °C together with the corresponding computer simulated spectra (above). Identification of the principal peaks of the superimposed powder spectra is indicated by p, the ring para position, α, the α-CD_2 group, and R, the ring ortho and meta positions.

al.[29,30] studied the influence of BZA on the capacitance of black lipid membranes formed from egg lecithin. It was found that the capacitance of the hydrocarbon region was reduced, suggesting a thickening of the bilayer. In contrast membranes formed in the absence of *n*-alkane solvent (commonly used to dissolve the lipid before painting the membranes) are reduced in thickness in the presence of BZA,[31,32] indicating that the earlier result reflected increased solvent retention by the bilayer. Metcalfe et al. studied the binding of BZA in erythrocyte membranes, lipid bilayers, and protein extracts.[33,34] Proton NMR studies of the choline methyl groups in model membranes indicate that a fraction of the dissolved BZA molecules exists within the interfacial region close enough to the choline moiety to cause aromatic ring current induced chemical shifts in the *N*-methyl protons.[35]

^2H NMR of selectively deuterated lipids has been extensively employed to study molecular orientational ordering and mobility in model membranes formed from both synthetic lipids and lipid extracts of biological membranes.[38,39] The ^2H NMR spectrum has the advantage of being little affected by intermolecular interactions and consequently its interpretation is relatively unambiguous. In addition, the method generates minimum perturbation to the system under study. The use of ^2H NMR in the study of solutes incorporated in lipid bilayers has been much more limited.[24-26,28,36,40-44] In order to further characterize the nature of anesthetic–membrane interactions in general, and that of BZA with lipid bilayers in particular, we have extended the work of Turner and Oldfield[36] by carrying out a ^2H NMR study of dimyristoylphosphatidylcholine (DMPC)/BZA/H_2O systems in which both the BZA and DMPC were selectively ^2H labeled. Deuterated BZA has several desirable features which make it a suitable compound for study in this way. In particular it contains a number of relatively rigid C–D bond directions which provide most of the information necessary to characterize its orientational ordering in the bilayer. Data from ^2H-labeled sites on the glycerol backbone and acyl chains of DMPC provide complementary information which assists in determining the disposition of the BZA molecule in the bilayer.

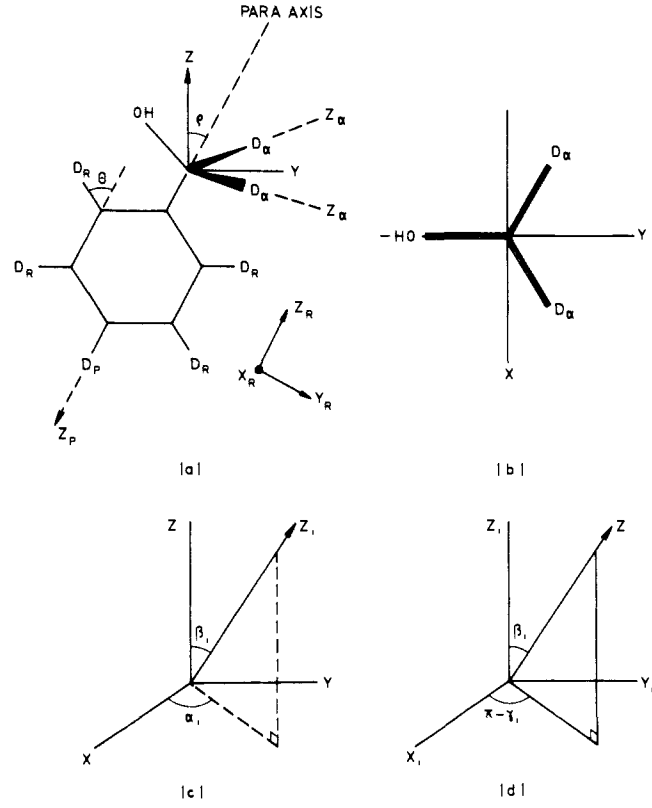

Figure 2. Illustration of the coordinate frames used in the text. (xyz) is the principal axis frame of the order matrix, ($x_iy_iz_i$) that of the individual sites in the molecule with i = p, α, and R corresponding to the para, α-CD_2, and ring (ortho and meta) deuterons, respectively, the latter chosen to take account of the ring flipping motion. A tetrahedral arrangement was assumed for the C–OH, C–D_α, and C–C (aromatic) bonds and the para axis chosen to lie in the yz plane of illustration (a). A view parallel to the para axis is shown in (b) while (c) and (d) illustrate the Euler angles ($\alpha_i\beta_i\gamma_i$) employed in the calculation.

Theory

The spectral patterns illustrated in Figure 1 are characteristic of uniaxially ordered molecules in which the deuterium quadrupole interaction has been averaged in the fast motion regime.[45] In this case, the splittings, $\Delta\nu_i$, between the edge singularities of the ith deuterated site are related to the time-averaged quadrupole interaction $\bar{\nu}_Q{}^i = e^2Q\bar{q}/h$ by the expression

$$\Delta\nu_i = \tfrac{3}{4}\bar{\nu}_Q{}^i \qquad (1)$$

where $e\bar{q} = \bar{V}_{z_Nz_N}$ is the principal (z_N) component of the time-averaged electric field gradient tensor (parallel to the bilayer normal) and eQ is the quadrupole moment of the nuclear spin.

Because some of the C–D bonds are differently oriented with respect to the most ordered axis of the molecule, the quadrupole

(32) Ebihara, L.; Hall, J. E.; MacDonald, R. C.; McIntosh, T. J.; Simon, S. A. *Biophys. J.* **1979**, *28*, 185–196.
(33) Metcalfe, J. C.; Seeman, P.; Burgen, A. S. V. *Mol. Pharmacol.* **1968**, *4*, 87–95.
(34) Colley, C. M.; Metcalfe, S. M.; Turner, G.; Burgen, A. S. V.; Metcalfe, J. C. *Biochim. Biophys. Acta* **1971**, *23*, 720–729.
(35) Colley, C. M.; Metcalfe, J. C. *FEBS Lett* **1972**, *24*, 241–246.
(36) Turner, G. L.; Oldfield, E. *Nature (London)* **1979**, *277*, 669–670.
(37) Shibata, T.; Sugiura, Y.; Iwayanagi, S. *Chem. Phys. Lipids* **1982**, *31*, 105–116.
(38) Seelig, J. *Q. Rev. Biophys.* **1977**, *10*, 353–418.
(39) Davis, J. H. *Biochim. Biophys. Acta* **1983**, *737*, 117–171.
(40) Stockton, G. W.; Smith, I. C. P. *Chem. Phys. Lipids* **1976**, *17*, 251–263.
(41) Oldfield, E.; Meadows, M.; Rice, D.; Jacobs, R. *Biochemistry* **1978**, *17*, 2727–2739.
(42) Valic, M. I.; Gorrissen, H.; Cushley, R. J.; Bloom, M. *Biochemistry* **1979**, *18*, 854–859.
(43) Taylor, M. G.; Akiyama, T.; Saito, H.; Smith, I. C. P. *Chem. Phys. Lipids* **1982**, *31*, 359–379.
(44) Dufourc, E. J.; Parish, E. J.; Chitrakorn, S.; Smith, I. C. P. *Biochemistry* **1984**, *23*, 6062.
(45) Doane, J. W. In *Magnetic resonance of phase transitions*; Owens, F. J., Poole, C. P., Farach, H. A., Eds.; Academic Press: New York, 1979; pp 171–246.
(46) Burnell, E. E.; de Lange, C. A. *Chem. Phys. Lett.* **1980**, *76*, 268–272.
(47) Zannoni C. In *Nuclear Magnetic Resonance of Liquid Crystals*; J. W. Emsley, J. W., Ed.; Reidel: New York, 1985.
(48) Ellis, D. M.; Bjorkstam, J. L. *J. Chem. Phys.* **1967**, *46*, 4460–4463.

interactions, which are almost entirely intramolecular in origin and determined by the electronic configuration of this bond, are differently averaged by the thermal motion. In order to compare the averaging of the various spectral components, a common procedure is to make use of the Maier–Saupe order tensor $S_{jk} = {}^1/_2\langle 3\cos\theta_j\cos\theta_k - \delta_{jk}\rangle$ $(j, k = x, y, z)$ where the θ_j define the instantaneous orientation of a coordinate frame fixed to the molecule, relative to the common z_N axis of the averaged field gradient tensor from all of the sites (in this case the bilayer normal). In its diagonal form, there are only two order parameters S_{zz} and $(S_{xx} - S_{yy})$ for the order matrix where x, y, z are the axes which diagonalize the matrix (the principal molecular axes). If α_i, β_i, and γ_i are the Euler angles (see Figure 2) that give the orientation of the principal axes of the field gradient tensor associated with a particular deuterated site relative to the principal molecular axes, the motion of the x, y, z frame due to thermal reorientation will, in the fast motion regime, yield an average coupling constant, $\bar{\nu}_Q{}^i$, given by the expression[45]

$$\bar{\nu}_Q{}^i = \nu_Q{}^i\left\{S_{zz}\left[\left(\frac{3}{2}\cos^2\beta_i - \frac{1}{2}\right) + \frac{\eta^i}{2}\sin^2\beta_i\cos 2\gamma_i\right] + (S_{xx} - S_{yy})\left[\frac{1}{2}\sin^2\beta_i\cos 2\alpha_i + \frac{\eta^i}{6}(1 + \cos^2\beta_i)\cos 2\alpha_i\cos 2\gamma_i - \frac{\eta^i}{3}\cos\beta_i\sin 2\alpha_i\sin 2\gamma_i\right]\right\} \quad (2)$$

where $\nu_Q{}^i$ and η^i are the coupling constant and asymmetry parameter, respectively, associated with the particular site prior to the averaging process. A common problem in these studies is that internal motion within the molecule causes an additional averaging. In general in such cases it is necessary to define a set of principal molecular axes and order parameters for each molecular conformation, unless these are rendered equivalent by the molecular symmetry.[46,47] However, in the limit that the conformational motion is independent of the molecular motion, the above analysis is still applicable provided $\nu_Q{}^i$ and η^i are replaced by quantities $\tilde{\nu}^i$ and $\tilde{\eta}^i$ respectively, which reflect this internal averaging.

In the application of eq 2 we have fixed the molecular x, y, z frame to the hydroxymethyl group as indicated in Figure 2a,b. Because the α-positions show equivalent spectra at all temperatures, we take the z, y plane to bisect the two C–D_α bonds. Not knowing the orientation of z we let it subtend an angle ρ (to be measured) relative to the para axis of the ring. Assuming a tetrahedral configuration for the C–OH, C–D_α, C–D_α, and C–C (ipso) bonds and using the principal axes associated with each site as indicated in Figure 2a, eq 2 gives

$$\bar{\nu}_Q{}^P = \nu_Q{}^P\left\{\left(\frac{3}{2}\cos^2\rho - \frac{1}{2}\right)S_{zz} - \frac{1}{2}(\sin^2\rho)(S_{xx} - S_{yy})\right\} \quad (3a)$$

$$\bar{\nu}_Q{}^\alpha = \nu_Q{}^\alpha\left\{\frac{1}{2}[\sin^2(35.26 - \rho) - 1]S_{zz} + \frac{1}{6}[\sin^2(35.26 - \rho) + 1](S_{xx} - S_{yy})\right\} \quad (3b)$$

$$\bar{\nu}_Q{}^R = \tilde{\nu}_Q{}^R\left\{\left[\left(\frac{3}{2}\cos^2\rho - \frac{1}{2}\right) - \frac{\tilde{\eta}^R}{2}\sin^2\rho\right]S_{zz} - \left[\frac{1}{2}\sin^2\rho - \frac{\tilde{\eta}^R}{6}(1 + \cos^2\rho)\right](S_{xx} - S_{yy})\right\} \quad (3c)$$

where the superscripts refer to the para, α-CD_2, and ring (ortho and meta) positions and the values of $\nu_Q{}^P$ and $\nu_Q{}^\alpha$ we take as 182 and 175 kHz, respectively.[39,48] Since in this case the ring can rotate relative to the hydroxymethyl group we must model this motion in order to use the splitting of the ortho and meta positions of the ring in the evaluation of molecular order. We are forced to do this since knowledge of the splittings from the α-CD_2 and para positions alone is insufficient to solve for the 3 unknown, ρ, S_{zz}, and $(S_{xx} - S_{yy})$. Accordingly we have calculated the average quadrupolar interaction at the ortho and meta ring positions on the basis of several possible models for the conformational motion.

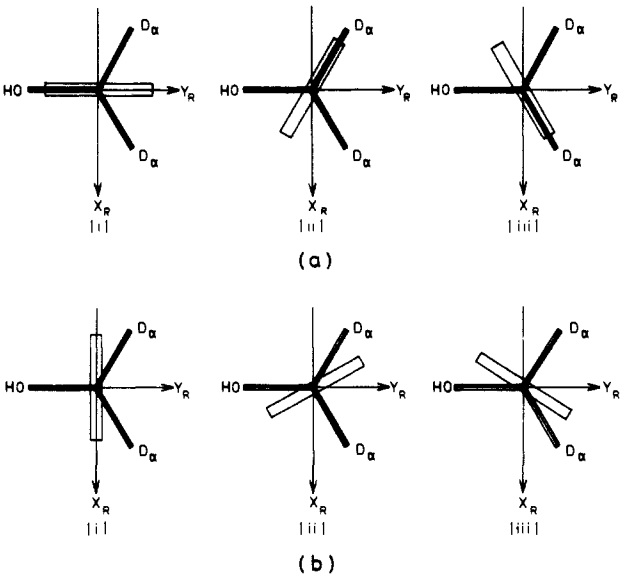

Figure 3. Possible conformations of the flipping aromatic ring, with $(x_R y_R z_R)$ the time averaged principal axes and z_R parallel to the para axis of the ring. The ring flip models illustrated include (a) the three conformations in which one of the C–D_α or C–O bonds lies in the plane of the ring. Conformation a(i) is assigned probability p, while that of a(ii) and a(iii) is $(1 - p)/2$ in each case. (b) The three conformations in which one of the C–D_α or C–O bonds is in a plane normal to that of the ring, with probabilities $(1 - p')/2$ and p', respectively.

Free Rotation Model. This is the model normally assumed for this motion.[49] Free rotation about the para-axis yields $\tilde{\nu}_Q{}^R = ({}^3/_2\cos^2\theta - {}^1/_2)\nu_Q{}^R$ where the angle, θ, between the C–D_α bond and the para axis is assumed to be 60° and $\nu_Q{}^R = 182$ kHz.[49] We shall show in the discussion, however, that this model yields unacceptable results.

Hindered Rotation Model. A more realistic model is one in which the ring prefers one of several conformations relative to the hydroxymethyl group such as those indicated in Figure 3. For rotation about the para axis and noting that x_R and y_R are axes of symmetry, the field gradient tensors in the x_R, y_R, z_R frame can be expressed as[50]

$$\begin{aligned} V_{x_Rx_R} &= V_{z_iz_i}({}^3/_2\sin^2\theta\cos^2\phi - {}^1/_2) \\ V_{y_Ry_R} &= V_{z_iz_i}({}^3/_2\sin^2\theta\sin^2\phi - {}^1/_2) \\ V_{z_Rz_R} &= V_{z_iz_i}({}^3/_2\cos^2\theta - {}^1/_2) \end{aligned} \quad (4)$$

where θ and ϕ are the polar and azimuthal angles giving the orientation of the ith C–D bond (z axis) of the ortho and meta ring positions relative to the x_R, y_R, z_R frame. We take $\theta = 60°$ and ϕ takes on values consistent with a particular model. Defining $\tilde{\nu}_Q{}^R = (eQ/h)\bar{V}_{z_Rz_R}$ and $\tilde{\eta}^R = (\bar{V}_{x_Rx_R} - \bar{V}_{y_Ry_R})/\bar{V}_{z_Rz_R}$ we find that for all the models described in the caption of Figure 3 $\tilde{\nu}_Q{}^R = -\nu_Q{}^R/8$ while the value of $\tilde{\eta}^R$ is model dependent. For a ring flipping between the conformations of Figure 3a with a probability p of being in conformation 3a(i) we obtain

$$\tilde{\eta}^R = \frac{27p - 9}{2} \quad (5a)$$

while for a similar 6-fold flip of the ring between the conformations of Figure 3b with probability p' assigned to conformation 3b(i)

$$\tilde{\eta}^R = \frac{-27p' - 9}{2} \quad (5b)$$

(49) Rowell, J. C.; Phillips, W. D.; Melby, L. R.; Panar, M. *J. Chem. Phys.* **1965**, *43*, 3442–3454.
(50) Vaz, N. A. P.; Vaz, M. J.; Doane, J. W. *Phys. Rev.* **1984**, *A30*, 1008–1016.

Table I. Calculated Values $\bar{\eta}^R$ for the Various Ring Flip Models Described in Figure 3[a]

	model	η^R
1.	(i) π and 120° flips of the ring between all conformations of Figure 3a	$(27p - 9)/2$
	(ii) π and 120° flips of the ring from conformations of Figure 3a (ii) and (iii) (p = 0)	$-9/2$
	(iii) π flips of the ring from conformation of Figure 3a (i) (p = 1)	$+9$
2.	(i) π and 120° flips of the ring between all conformations of Figure 3b	$(-27p' + 9)/2$
	(ii) π and 120° flips of the ring from conformations of Figure 3b (ii) and (iii) (p' = 0)	$+9/2$
	(iii) π flips of the ring from conformation of Figure 3b (i) (p' = 1)	-9

[a] Note: In all cases $\bar{\nu}_Q^R = -\nu_Q^R/8 = -22.75$ kHz. Values for $\bar{\eta}^R$ assume $\theta = 60°$ (Figure 2a). The value of p or p' predicts the probability of the conformers of Figure 3a (i) and Figure 3b (i), respectively. The remaining conformers in each group then have probability $(1 - p)/2$ or $(1 - p')/2$. Free rotation of the ring corresponds to p or $p' = {}^1/_3$.

Results for some specific cases are summarized in Table I. It may be noted that the values of $\bar{\eta}^R$ may be greater than one or negative which simply indicates that we have not followed the convention of taking $|\bar{V}_{x_Rx_R}| \leq |\bar{V}_{y_Ry_R}| \leq |\bar{V}_{z_Rz_R}|$.

The above analysis is valid subject to the conditions indicated above, that the conformational motion of the ring is independent of the orientation of the molecule in the bilayer. A further approximation, commonly employed in studies of molecular order in lipid crystal systems,[45] is to assume that $(S_{xx} - S_{yy}) = 0$, enabling eq 3a and 3b to be solved for ρ and S_{zz} independent of a model for the ring motion.

Materials and Methods

Synthesis of ^{2}H-Labeled Fatty Acids. 14,14,14-Trideuteriotetradecanoic (myristic) acid was prepared by the method of Westerman and Ghrayeb.[51] 6,6-Dideuteriotetradecanoic acid was synthesized by anodic coupling of α-deuterated decanoic acid with monomethylsuccinate.[41] Deuterium exchange at the α-position of myristic and decanoic acids was accomplished by using a modification of the method of Aasen et al.[52] The purity of the ^{2}H-labeled fatty acids was confirmed by GLC of the corresponding methyl esters. GLC was performed on a Hewlett-Packard 5840 gas chromatograph with a column packed with 10% Silar-10C on 100–120 mesh gas Chrom Q. The position and extent of isotropic incorporation of the ^{2}H labels were determined by ^{13}C NMR and mass spectrometry. Natural abundance ^{13}C NMR spectra (15% (w/v) solutions in $CHCl_3$) were obtained on either Bruker WP 80 or Varian FT80 spectrometers operating at 20.115 MHz with proton noise decoupling.

Synthesis of ^{2}H-Labeled Dimyristoylphosphatidylcholine. DMPC, selectively ^{2}H-labeled on the *sn*-2 acyl chain was prepared by the following sequence of reactions. Glycerophoshocholine cadmium chloride (GPC·$CdCl_2$), prepared from egg lecithin, was acylated with unlabeled myristic acid anhydride to yield 1,2-dimyristoyl-*sn*-glycero-3-phosphocholine.[41] Enzymatic removal of the fatty acid from the *sn*-2 position[53] gave lysolecithin, which was then acylated with either ^{2}H-labeled myristic acid[54] or ^{2}H-labeled myristic acid anhydride[55] to yield labeled 1,2-diacyl-*sn*-glycero-3-phosphocholine. The product was isolated by column chromatography on silica gel, eluting with chloroform/methanol 8:2 or 7:3 (v/v). TLC analyses were carried out on Absorbosil-5 silica gel plates (Applied Sciences), using chloroform/methanol/water 65:25:4 (v/v) as the solvent system and both molybdenum blue and iodine vapor to visualize spots. The positional purity of the phosphatidylcholine was determined by GLC and mass spectral analysis of the fatty acids as methyl esters after hydrolysis with phospholipase A_2.[56] Phosphate analyses were performed by the method of McClare.[57] DMPC selectively ^{2}H-labeled on the 2′ positions of both the *sn*-1 and *sn*-2 chains was prepared by acylation of GPC·$CdCl_2$.[54]

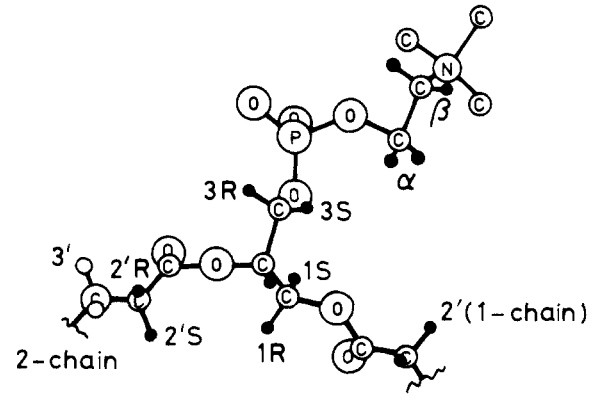

Figure 4. The structure of dimyristoylphosphatidylcholine (DMPC) indicating the selectivity ^{2}H-labeled sites in the region of the headgroup and glycerol backbone.

Selective deuteration of the glycerol moiety was achieved by the following procedure. *rac*-Isopropylidene [2-^{2}H]glycerol was prepared by reduction of dihydroxyacetone with NaB^2H_4[58] and *rac*-isopropylidene [1,3-$^2H_4$]glycerol was synthesized from diethylacetoxymalonate by reduction with $LiAl^2H_4$.[58] The appropriately labeled *rac*-isopropylidene glycerol was used to prepare in several steps selectively deuterated 1,2-dimyristoyl-*rac*-glycerol,[59] which was then converted to ^{2}H-labeled DMPC by the procedure of Eibl.[60] DMPC selectively deuterated on the choline moiety was prepared by the same procedure utilizing ^{2}H-labeled ethanolamine[61] at the appropriate step. The positions of the labeled sites on the glycerol backbone and headgroup regions of the DMPC molecule are illustrated in Figure 4.

Synthesis of ^{2}H-Labeled Benzyl Alcohols. Reduction of methyl benzoate (Aldrich) with $LiAl^2H_4$ gave a quantitative yield of BZA(d_2), ^{2}H-labeled on the benzylic (α-CD_2) position. Purification by vacuum distillation produced material with physical properties consistent with published data. BZA both perdeuterated (d_7) and selectively deuterated on the benzene ring (d_5) were purchased from MSD (Merck, Sharp and Dohme) as isotopes and used without further purification. Benzyl alcohol, ^{2}H-labeled in the para position, was prepared from [4-^{2}H]benzoic acid by esterification and reduction with $LiAl^2H_4$. The labelled benzoic acid was synthesized by the treatment of *p*-chlorobenzoic acid with Raney nickel in ^2H_2O under alkaline conditions according to Buu-Hoi et al.[62]

Sample Preparation and Data Acquisition. The purity of phospholipid samples was checked by TLC both before and after recording NMR spectra. The DMPC/*n*BZA/9H_2O samples (with n = 0.1 and 0.5) were prepared by adding the appropriate quantities of labeled BZA and water to a weighed (~100 mg) amount of vacuum dried DMPC (Sigma) via a microsyringe in a test tube with a ~1-mm constriction. The tubes were then sealed with the contents frozen by dipping the end of the tube in liquid nitrogen and mixed by repeated centrifugation through the constriction.[28] Hydration of the ^{2}H-labeled DMPC samples was achieved by warming at 30 °C in excess deuterium depleted water (70–80% (w/w)) with thorough mixing.[63] Spectra from the ^{2}H-labeled BZA samples were recorded on a Bruker CXP 300 NMR spectrometer operating at 46.063 MHz, while those from the labeled DMPC were obtained at 30.87 MHz on a "home built" spectrometer. In both cases a quadrupolar echo technique was employed with cyclops phase cycling.[39] Low-angle X-ray diffraction patterns were obtained by using copper Kα radiation from a Hilger microfocus X-ray generator fitted with Elliot toroidal optics. Further details of sample preparation and analysis, instrumentation, and temperature control are contained in ref 28 and 63.

(51) Westerman, P. W.; Ghrayeb, N. *Chem. Phys. Lipids* **1981**, *29*, 351–358.
(52) Aasen, A. J.; Lauer, W. M.; Holan, R. T. *Lipids* **1970**, *5*, 869–877.
(53) Chakrabarti, P.; Khorana, H. G. *Biochemistry* **1975**, *14*, 5021–5033.
(54) Hermetter, A.; Paltauf, F. *Chem. Phys. Lipids* **1981**, *28*, 111–115.
(55) Gupta, C. M.; Radhakrishnan, R.; Khorana, H. G. *Proc. Natl. Acad. Sci. U.S.A.* **1977**, *74*, 4315–4319.
(56) van Deenen, L. L. M.; de Haas, G. H. *Biochim. Biophys. Acta* **1963**, *70*, 538–553.
(57) McClare, C. W. F. *Anal. Biochem.* **1971**, *39*, 527–530.
(58) Wohlgemuth, R.; Waespe-Sarcevic, N.; Seelig, J. *Biochemistry* **1980**, *19*, 3315–3321.
(59) Howe, R. J.; Malkin, T. *J. Chem. Soc.* **1951**, 2663–2667.
(60) Eibl, E. *Chem. Phys. Lipids* **1980**, *26*, 239–247.
(61) Taylor, M. G.; Smith, I. C. P. *Chem. Phys. Lipids* **1981**, *28*, 119–138.
(62) Buu-Hoi, N. P.; Dat Xuong, N.; van Bac, N. *Bull. Soc. Chim. Fr.* **1963**, 2442–2445.
(63) Westerman, P. W.; Vaz, M. J.; Strenk, L. M.; Doane, J. W. *Proc. Natl. Acad. Sci. U.S.A.* **1982**, *79*, 2890–2894.
(64) Katz, Y.; Diamond, J. M. *J. Membr. Biol.* **1974**, *17*, 101–120.

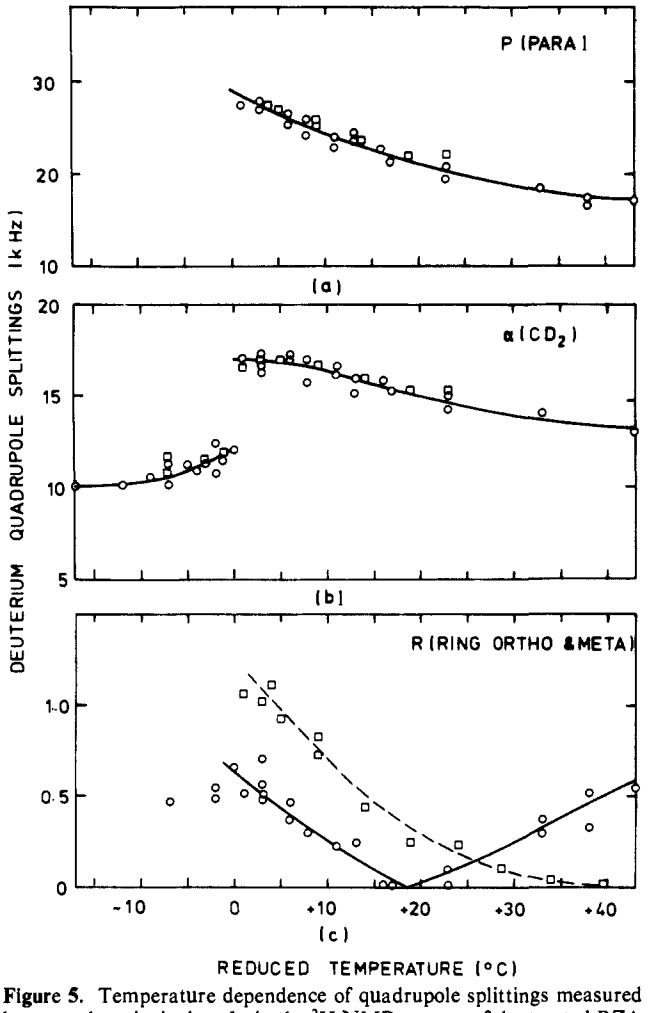

Figure 5. Temperature dependence of quadrupole splittings measured between the principal peaks in the ^2H NMR spectra of deuterated BZA in bilayer membranes formed from DMPC. The results are plotted against reduced temperature ($T - T_m$), where T_m is the main gel–liquid crystal transition temperature. Sample compositions are (○) DMPC/0.1 BZA/9H_2O (T_m = 24 °C) and (□) DMPC/0.5BZA/9H_2O (T_m = 18 °C). The full curves represent smoothed data for DMPC/0.1BZA/9H_2O as used in the theoretical analysis.

Results

Representative spectra for BZA(d_7) in bilayers of molar composition DMPC/0.5BZA/9H_2O are shown in Figure 1, together with the corresponding computer simulated (η = 0) powder spectra at two temperatures. The assignments of the principal peaks indicated in the figure were determined by comparison with similar results for BZA selectively deuterated at the para position of the ring and α-CD_2 positions, respectively. They were confirmed on the basis of the peak intensities required for the spectral simulations and a chemical shift of approximately 3–4 ppm between the center of the α-CD_2 component and that of the two components from the ring positions. The variation with temperature of the splittings between the principal peaks corresponding to para, α-CD_2, and ring (ortho and meta) deuterons is shown in Figure 5 for all samples studied. The results are plotted against reduced temperature ($T - T_m$) where T_m is the temperature of the main gel–liquid crystal transition. The latter is reduced on increasing both water and BZA concentration and was determined from the observed discontinuities in ^2H splittings at the transition. Values of T_m for the samples studied are given in the caption to Figure 5. Results shown include data from perdeuterated BZA(d_7) and BZA selectively deuterated at the ring (d_5) and α-CD_2 (d_2) positions.

It was found necessary to work at reduced hydration with the ^2H-labeled BZA samples in order to resolve the splittings from the ring ortho and meta deuterons (Figure 1). This also resulted in an improved signal-to-noise ratio, enabling us to work at concentrations (n = 0.1) approaching those employed for anesthesia. The samples at n = 0.5 were used mainly for spectral simulation purposes in order to check the peak assignments. In excess water the splittings from the α-CD_2 and para deuterons were reduced by approximately 15–20% at equivalent temperatures with respect to those obtained at reduced hydration.

Table II. Effects of Benzyl Alcohol on ^2H NMR Quadrupole Splittings of Specifically ^2H-Labeled DMPC[a]

position of ^2H label	quadrupole splittings (kHz)[b]	effect of benzyl alcohol[c]
3*S* (glycerol)	28.3	−1.5
3*R* (glycerol)	26.3	−1.3
2 (glycerol)	25.4	−0.1
1*R* (glycerol)	19.0	+0.6
1*S* (glycerol)	0.0	0.0
2′*R*,*S* (*sn*-1-chain)	26.0	+1.4
2′*R* (*sn*-2-chain)	17.5	+1.1
2′*S* (*sn*-2-chain)	12.4	+0.4
6′*R*,*S* (*sn*-2-chain)	26.8	+0.3
14′,14′,14′ (*sn*-2-chain)	3.0	−0.2
α-CH_2 (choline)	6.0	−0.6
β-CH_2 (choline)	4.9	−0.9

[a] For $T = T_m + 14$ °C; mol of BZA/mol of DMPC = 7/15 in bilayer. Ratio calculated using a DMPC/H_2O partition coefficient of 13.9.[64] [b] Multilamellar dispersion of pure DMPC in excess H_2O, for which chain melting temperature T_m = 23 °C. Error estimated to be ±0.2 kHz. [c] Positive value indicates an increase in the quadrupole splitting. For this sample, chain melting temperature T_m = 16 °C.

Results for the influence of BZA on the temperature variation of ^2H splittings from selectively deuterated DMPC in excess water are shown in Figure 6 and summarized in Table II for a temperature of 37 °C. In assigning quadrupole splittings in the ^2H NMR spectra of DMPC deuterated at the 1*R*, 1*S*, 3*R*, and 3*S* sites of the glycerol moiety it was assumed that these splittings in DMPC were very similar to values reported for the same positions in DMPC[65] dipalmitoylphosphatidylcholine,[66] and other phospholipids.[58,67,68] Stereospecific monodeuteration of several of these phospholipids showed that the two splittings from the 1-glycerol segment and the two splittings from the 3-glycerol segment reflect motional inequivalence of the individual deuterons.[67] Assignment of quadrupole splittings for DMPC, ^2H-labeled in the 2′ positions of the *sn*-1 and *sn*-2 chains, was based on reported values for these splittings.[69,70] α and β-CH_2 choline data were obtained on tetradeuterated material, and assignments are based on previously published data.[66,71]

Low-angle X-ray diffraction data from DMPC/BZA/11H_2O as a function of the concentration of BZA in the bilayer, above the phase transition, are shown in Figure 7. The thickness of the acylglycerol region (d_{AG}) and the bilayer area per phospholipid (A) were calculated from the bilayer repeat distance (d) according to the method of ref 28.

Discussion

In interpreting the data from ^2H-labeled BZA (Figure 5), two problems arise. Firstly, the ^2H NMR spectra yield the magnitudes of the time averaged quadrupole interactions $\bar{\nu}_Q^i$ for each labeled site i on the molecule from eq 1, but not their relative signs. Secondly, solution of eq 3a–c to yield values for ρ, S_{zz}, and ($S_{xx} - S_{yy}$) requires a knowledge of the ring motion relative to the hydroxymethyl group in order to obtain a value for $\bar{\eta}^R$ (see Table I). However, even in the absence of such information some progress can be made.

(65) Strenk, L. M.; Westerman, P. W.; Doane, J. W. *Biophys. J.* **1985**, *48*, 765–773.
(66) Gally, H. U.; Niederberger, W.; Seelig, J. *Biochemistry* **1975**, *14*, 3647–3652.
(67) Gally, H. U.; Pluschke, G.; Overath, P.; Seelig, J. *Biochemistry* **1981**, *20*, 1826–1831.
(68) Browning, J. L.; Seelig, J. *Biochemistry* **1980**, *19*, 1262–1270.
(69) Engel, A. K.; Cowburn, D. *FEBS Lett.* **1981**, *126*, 169–171.
(70) Seelig, J.; Seelig, A. *Q. Rev. Biophys.* **1980**, *13*, 19–61.
(71) Seelig, J.; Gally, H.; Wohlgermuth, R. *Biochim. Biophys. Acta* **1977**, *467*, 109–119.

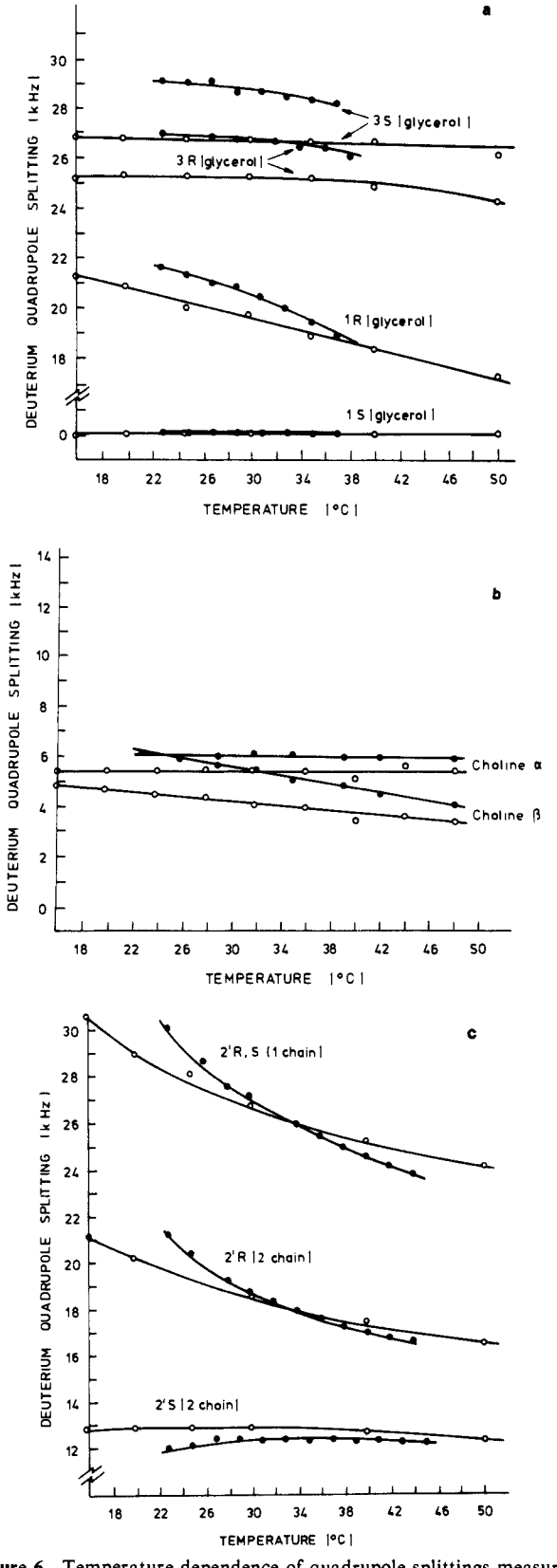

Figure 6. Temperature dependence of quadrupole splittings measured between the principal peaks in the ^2H NMR spectra of DMPC (●) and DMPC/BZA (○) (15 mol:7 mol) bilayer membranes in which the DMPC is ^2H-labeled (a) on the 1*R*,*S* and 3*R*,*S* positions of the glycerol backbone; (b) on the α and β (to the phosphate) methylene segments of the choline headgroup, and (c) on the 2′-positions of the *sn*-1 and -2 chains.

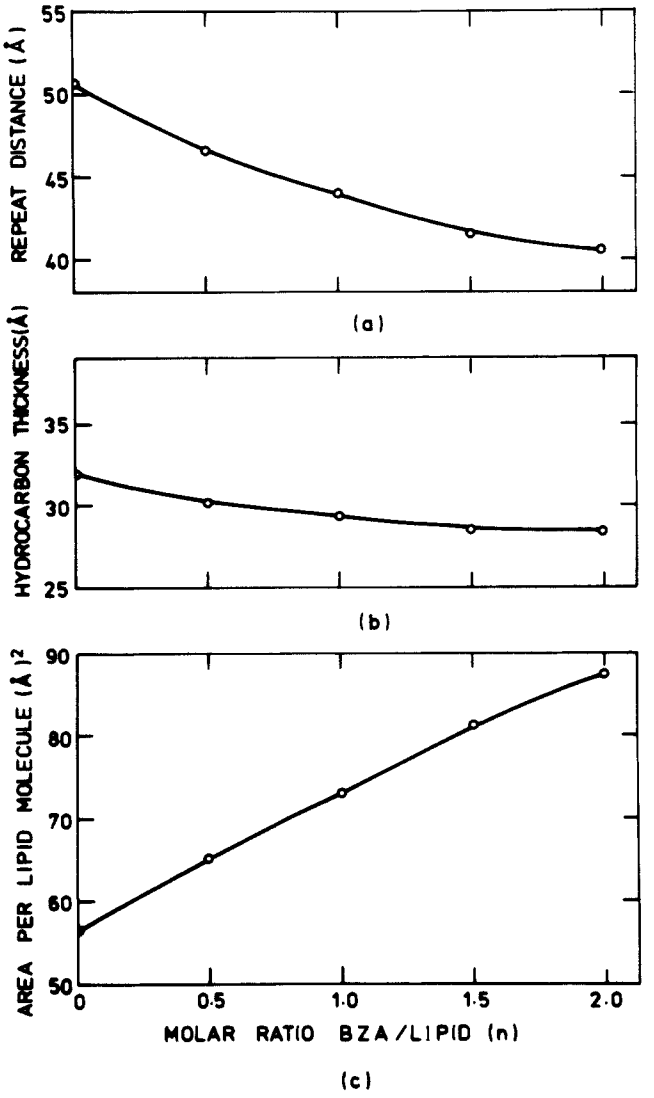

Figure 7. Variation with benzyl alcohol concentration of (a) the bilayer repeat distance *d*, (b) the thickness of the hydrocarbon region (acyl-glycerol region) d_{AG}, and (c) the bilayer area per lipid molecule A for bilayers of composition DMPC/BZA/11H_2O at a temperature just above the gel–liquid crystal phase transition, as determined by low-angle X-ray diffraction.

Firstly, a ring freely rotating about the para axis can be ruled out. From Table I free rotation ($p = {}^1/_3$ or $p' = {}^1/_3$) yields $\tilde{\eta}^R = 0$. Since in this case $\tilde{\nu}_Q{}^R = \nu_Q{}^R({}^3/_2 \cos^2\theta - {}^1/_2)$, where θ is the angle between the ortho and meta C–D bond directions relative to the para axis, we have from eq 3 with $\tilde{\eta}^R = 0$ that $\tilde{\nu}_Q{}^R/\nu_Q{}^P = ({}^3/_2 \cos^2\theta - {}^1/_2)$. The data of Figure 5 then clearly yield the unacceptable result that $\theta = 54.7°$ for BZA in DMPC/0.1BZA/9H_2O at $T_m + 18$ °C = 42 °C for which temperature $\tilde{\nu}_Q{}^R$ passes through zero. To satisfy this relationship θ would also have to vary by 2° in angle over the ~40 °C temperature range of our liquid crystal phase data. The value of θ however is known to be 60° ± 1° and would would not be expected to vary with temperature in this way.[49]

The fact that the ^2H splittings for the ring positions of BZA pass through zero in the temperature range of our data also removes much of the uncertainty over the relative signs of the observed ^2H splittings. For this temperature there are then only two possibilities—corresponding to the time averaged quadrupole interactions for the α-CD_2 and para deuterons having the same or opposite signs. Consequently we have sought solutions to eq 3 at this temperature for DMPC/0.1BZA/9H_2O, over the full range of the weighting parameter *p*, viz $0 \le p \le 1$ for the 6-fold flip model of Figure 3a. The solutions were found by substituting for S_{zz} from eq 3a and 3b and 3c and rearranging to obtain two separate expressions for $(S_{xx} - S_{yy})$ in terms of ρ, *p*, and the measured splittings. For a given *p* value, these expressions were then compared over a suitable range of ρ values ($-90° \le \rho \le$

+90°). For values of ρ which gave simultaneous solutions for $(S_{xx} - S_{yy})$, all three order parameters S_{xx}, S_{yy}, and S_{zz} were calculated by making use of the identity $S_{xx} + S_{yy} + S_{zz} = 0$. Apparent "solutions" for ρ which yielded values of the maximum order parameter (largest of S_{xx}, S_{yy}, and S_{zz}) $S_{MAX} > 1$ were discarded, as were those for which any two of the S_{ii}'s had magnitudes >0.5, this being inconsistent with the above identity and the definition of the order parameters which requires $-0.5 \leq S_{ij} \leq 1$. Clearly, from eq 5a and 5b, a solution corresponding to a particular p value can in general also be interpreted in terms of the alternative 6-fold flip model of Figure 3b with $p' = 2/3 - p$, subject of course to the proviso that $0 \leq p' \leq 1$.

The solutions are illustrated in Figure 8a–c. We have defined D/S as the difference between the two smaller components of the order matrix (D) divided by the largest component S_{MAX}. For the case where the α-CD_2 and para deuteron splittings were assumed to be of opposite sign (case A), there are no solutions for p values in the range $0.26 \lesssim p \lesssim 0.38$. For $p = 0$ and low values of this parameter the most ordered axis is z (Figure 2a). While with $p \simeq 0.11$, $|D/S| \rightarrow 1$ and the most ordered axis switches to y in the range $0.11 \lesssim p \lesssim 0.26$ and $0.38 \lesssim p \lesssim 0.4$. For $0.4 \lesssim p \lesssim 0.51$ there is a further change of the most ordered axis to x, before returning to z for $p > 0.51$. However, for the most ordered axis to be x requires that this axis be parallel to the bilayer normal. This would appear to be unlikely if, as anticipated, the polar hydroxyl group of BZA confers on the molecule a preference for the aqueous interface region of the bilayer, since such a conformation could be expected to result in maximum disruption of the bilayer structure. That the BZA molecule does reside preferentially in the vicinity of the lipid headgroups and glycerol backbone region of the bilayer is confirmed by our X-ray diffraction data and NMR results for bilayers comprising ^{2}H-labeled DMPC (see below).

If the time averaged quadrupole interactions for the α-CD_2 and para deuterons are assumed to have the same sign (case B), solutions can be found only for p values $\lesssim 0.3$. Here the y axis is most ordered for $0 \lesssim p \lesssim 0.11$ and $0.27 \lesssim p \lesssim 0.3$, but it switches to z in the intervening range.

With the exception of a narrow range of p values ($0.22 \lesssim p \lesssim 0.26$ and $0.38 \lesssim p \lesssim 0.385$ for case A and $0.285 \lesssim p \lesssim 0.30$ for case B), values of the order parameter for the most ordered axis (S_{MAX}) are restricted to the ranges $0.18 \lesssim S_{MAX} \lesssim 0.5$ and $0.39 \lesssim S_{MAX} \lesssim 0.5$, respectively. To further restrict the range of possible solutions would require a knowledge of either the ring motion or the relative signs of the quadrupole couplings for the various sites, derived from some independent measurement. On the basis of gas electron diffraction,[72] infrared spectroscopy,[73] NMR spectroscopy,[74] and molecular force field calculations,[73] exchange models of the type illustrated in Figure 3 appear to be favored. Experimental evidence[72,74] indicates that the dominant conformation corresponds either to a C_{Ar}–C torsion angle of approximately 60° [conformers 3a (ii) and (iii) of Figure 3, i.e., $p \rightarrow 0$] or free rotation of the ring around this bond. In contrast the molecular force field calculations[73] appear to favor slightly the conformation of Figure 3b (i), but this conformation is not supported by the NMR data.[74] Since the experimental data for the gas phase and solutions of BZA in both CCl_4 and Me_2SO point to p values close to zero, we have calculated values of ρ, S_{MAX}, and $|D/S|$ for DMPC/0.1BZA/9H_2O over the full temperature range of our measurements. Results are shown in Figure 9, together with similar results obtained on the assumption $D = (S_{xx} - S_{yy}) = 0$ for comparison. The p values corresponding to these solutions are $p \approx 0.78$ (case A) and $p \approx 0.27$ or $p' \approx 0.40$ (case B) almost independent of temperature over the range studied. The bars on the points in Figure 9 indicate the separation of values obtained on the assumption of positive or negative sign respectively for the time averaged quadrupole interaction for the ring (ortho

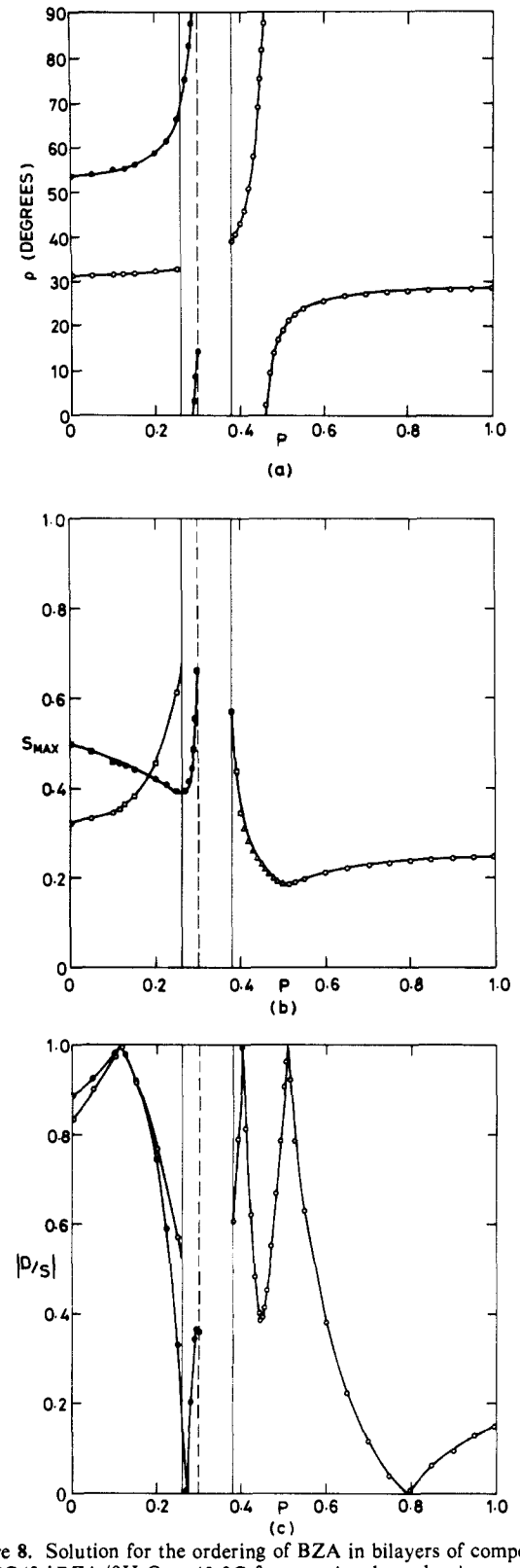

Figure 8. Solution for the ordering of BZA in bilayers of composition DMPC/0.1BZA/9H_2O at 42 °C for case A, where the time averaged quadrupole interactions at the α-CD_2 and para sites ($\bar{\nu}_Q^{\alpha}$ and $\bar{\nu}_Q^{P}$, respectively) are assumed to have opposite sign (open symbols) and case B where they are assumed of the same sign (full symbols). The plots show the variation with statistical weighting parameter p (which describes the motion of the ring with respect to the α-hydroxymethyl group) of (a) the angle ρ which defines the orientation of the principal molecular axes with respect to the molecule, (b) the magnitude of the largest diagonal component of the ordering matrix, S_{MAX}, and (c) the quantity $|D/S|$, defined as the modulus of the difference between the other two diagonal components divided by S_{MAX}. In b the symbols indicate (○, ●) $S_{MAX} \equiv S_{zz}$, (□, ■) $S_{MAX} \equiv S_{yy}$, and (△) $S_{MAX} \equiv S_{xx}$. There are no solutions for $0.26 \lesssim p \lesssim 0.38$ (case A) or $p \gtrsim 0.3$ (case B).

(72) Traetteberg, M.; Oestersen, H.; Seip, R. *Acta Chem. Scand.* **1980**, *A34*, 449–454.
(73) Ito, M.; Hirota, M. *Bull. Chem. Soc. Jpn.* **1981**, *54*, 2093–2098.
(74) Abraham, R. J.; Bakka, M. *Tetrahedron* **1978**, *34*, 2947–2951.

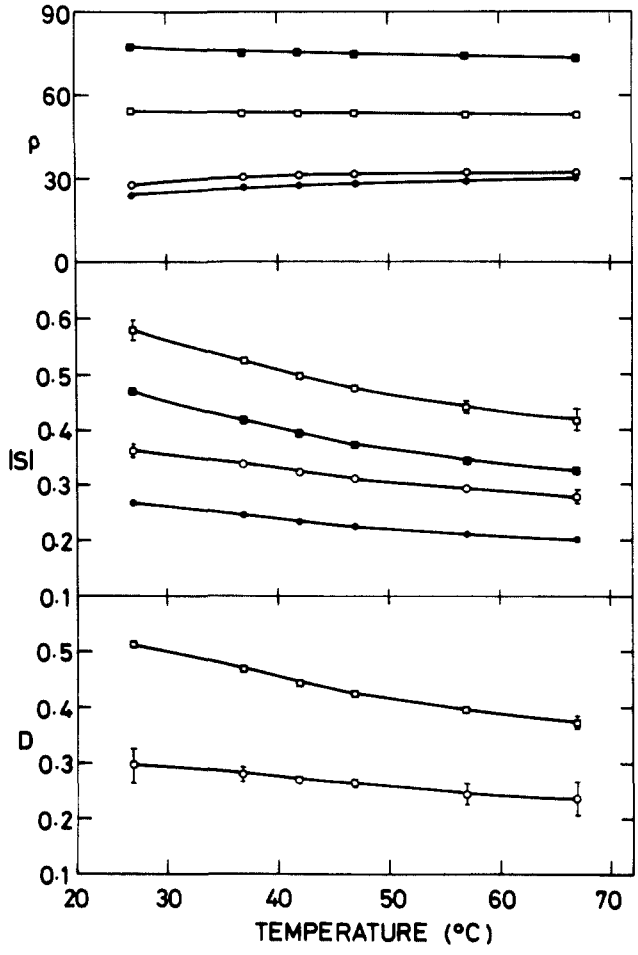

Figure 9. Variation with temperature of the orientation of the principal molecular axes with respect to the molecule ρ and order parameters S_{zz} and $D = S_{xx} - S_{yy}$ for BZA in bilayers of composition DMPC/0.1BZA/9H_2O. The data refer to the case $p = 0$ corresponding to the conformations of Figure 3a (ii) and (iii) (open symbols) and the solutions obtained by assuming $D = 0$ (full symbols). (○, ●) $\tilde{\nu}_Q^{\alpha}$ and $\tilde{\nu}_Q^{P}$ assumed to have opposite sign (case A); (□, ■) $\tilde{\nu}_Q^{\alpha}$ and $\tilde{\nu}_Q^{P}$ assumed to have the same sign (case B). The bars on the symbols indicate the difference between values obtained on the assumption of positive and negative signs for $\tilde{\nu}_Q^{R}$ with respect to $\tilde{\nu}_Q^{P}$, respectively.

and meta) deuterons $\tilde{\nu}_Q^{R}$ with respect to $\tilde{\nu}_Q^{P}$. Obviously there is no distinction between these cases in the vicinity of 42 °C where the ring deuteron splittings pass through zero. It is tempting to reject solutions with $S_{MAX} \gtrsim 0.5$ on the basis that molecular order parameters (S_{mol}) for the most ordered sites on the lipid molecules themselves are below this value.[38,39,75] This would suggest that solutions with $\tilde{\nu}_Q^{\alpha}$ opposite in sign to $\tilde{\nu}_Q^{P}$ should be favored (Figure 9). However, it should be remembered that values of S_{mol} include the effects of lipid conformational motion in addition to the reorientation of the molecular long axis which might be expected largely to influence the order of a BZA solute molecule. We emphasize also that the above analysis assumes "ideal" molecular geometry.

In comparing results for samples of different composition, it is noticeable that an increase in the molar ratio of BZA to lipid from 0.1 to 0.5 at the same water content has negligible effect on the splittings for the α-CD_2 and para deuterons, at a given value of reduced temperature ($T - T_m$), affecting only those for the ring ortho and meta sites (Figure 5). Since the latter only are influenced by the conformational motion, this suggests that the main effect of changing BZA concentration is to change the parameter p which describes the statistical weight of the various possible conformations. In contrast the effect of increasing lipid hydration may be to reduce bilayer order to an extent greater than can be explained purely in terms of the reduction in chain melting temperature.

Information on the location of BZA in the bilayer and its effect on bilayer order can be inferred from studies of bilayers formed from ^{2}H-labeled lipids (Figure 6), together with low-angle X-ray diffraction data (Figure 7). Largest effects on lipid ^{2}H splittings on incorporation of BZA at constant reduced temperature ($T - T_m$) are observed at the 3*R* and 3*S* positions of the glycerol backbone, the choline α and β positions (for all of which BZA produces a decreased splitting), and the 2′*R*,*S* positions of the *sn*-1 chain and 2′*R* position on the *sn*-2 chain, for which the splittings increase on incorporation of BZA (Table II). This is consistent with a strong interaction between DMPC and BZA in the region of the glycerol bridge and the top of the alkyl chains, the presence of the BZA molecules causing increased order in this region of the bilayer. There is some evidence that the ordering effect of BZA on the bilayer may extend down to the 6′ position of the alkyl chains, but the effect is one of a slight disordering at the methyl terminal. This effect and the reduced order at the glycerol 3*R*,*S* and choline α and β positions can be readily explained as a consequence of the lipid molecules being forced apart by the presence of the BZA solute, giving rise to an increase in bilayer area. This in turn will result in greater reorientational freedom for the headgroup, while the ends of the chains must disorder to take up this additional bilayer area. It should be noted that our data for the 6′ position of the *sn*-2 chain are not inconsistent with the results of Turner and Oldfield,[34] who reported a reduction in order for this position in the presence of BZA at constant temperature. We believe that comparison of the splittings at fixed reduced temperature ($T - T_m$) is more revealing. Note also that while the presence of BZA in the bilayer reduces ^{2}H splittings at the 3*R* and 3*S* sites, they still have inequivalent splittings. We have found that the presence of a number of other bilayer solutes chemically related to BZA, such as butanol and octanol, also reduces the splittings at these sites without destroying their nonequivalence (unpublished results).

The low-angle X-ray data of Figure 7 confirm that BZA resides preferentially at the aqueous interface region of the lipid bilayer, giving rise to substantial increase in bilayer area with increasing BZA concentration. This increase in area per lipid molecule in turn results in some disordering of the lipid chains to fill space in interior of the bilayer, with a consequent small reduction in bilayer thickness. Note that significant changes in bilayer area can be expected even at pharmacological concentrations of BZA (of order 0.1 molar in the bilayer).

In summary our results show that BZA is located principally in the aqueous interface region of the lipid bilayer. Its incorporation at concentrations comparable to those known to induce anaesthesia produces appreciable changes in bilayer structure and molecular order. A number of models for the ordering and conformational motion of the BZA within the lipid bilayer have been explored and the principal components of the molecular ordering matrix derived for several of these models. A model in which the benzene ring reorients freely with respect to the α-hydroxymethyl group about the para axis is not consistent with the observed results.

Acknowledgment. We are grateful to Sutin Horvath for synthesizing specifically ^{2}H-labeled DMPCs and benzyl alcohols. We also acknowledge Nason Phonphok and Leonard Walker for recording several ^{2}H NMR spectra. This work was supported in part by the National Institutes of Health (GM27127) and by the Australian Research Grants Scheme.

Registry No. BZA, 100-51-6.

(75) Gruen, D. W. R. *Chem. Phys. Lipids* **1982**, *30*, 105–120.